On the Azo/Hydrazo Equilibrium in Sudan I Azo Dye Derivatives

ARTICLE *in* THE JOURNAL OF PHYSICAL CHEMISTRY A · JANUARY 2013

Impact Factor: 2.69 · DOI: 10.1021/jp310229h · Source: PubMed

5 AUTHORS, INCLUDING:

Hélio F. Dos Santos
Federal University of Juiz de Fora
135 PUBLICATIONS **1,412** CITATIONS
SEE PROFILE

Luiz Fernando Cappa De Oliveira
Federal University of Juiz de Fora
175 PUBLICATIONS **1,758** CITATIONS
SEE PROFILE

THE JOURNAL OF PHYSICAL CHEMISTRY A

Article

pubs.acs.org/JPCA

On the Azo/Hydrazo Equilibrium in Sudan I Azo Dye Derivatives

Gilson R. Ferreira,[†,‡] Humberto Costa Garcia,[†] Mara Rubia C. Couri,[†] Hélio F. Dos Santos,[‡] and Luiz Fernando C. de Oliveira*[,†]

[†]Núcleo de Espectroscopia e Estrutura Molecular (NEEM), and [‡]Núcleo de Estudos em Química Computacional (NEQC), Departamento de Química, Universidade Federal de Juiz de Fora, Juiz de Fora, MG, 36036-330, Brazil

Supporting Information

ABSTRACT: In this study, Raman, infrared, UV/vis, NMR, and single crystal X-ray diffraction spectroscopies are used to elucidate the tautomeric equilibrium of azo dyes derived from 1-phenyl-azo-2-naphthol (Sudan I). A new crystallographic structure is described for Sudan I, revealing the presence of intramolecular hydrogen bonds and supramolecular interactions, such as the unconventional C−H···O hydrogen bond type, π-stacking, and charge−dipole interactions. All of these weak intermolecular interactions play a role in the stability of the crystalline structure. Theoretical calculations are also reported for geometries, energy, and spectroscopic properties. The predicted spectra are in accordance with the experiments carried out in the solid state and in solution of dichloromethane, carbon tetrachloride, and chloroform, suggesting the hydrazo form as the preferable tautomer in gas and condensate phases for Sudan I and its derivatives.

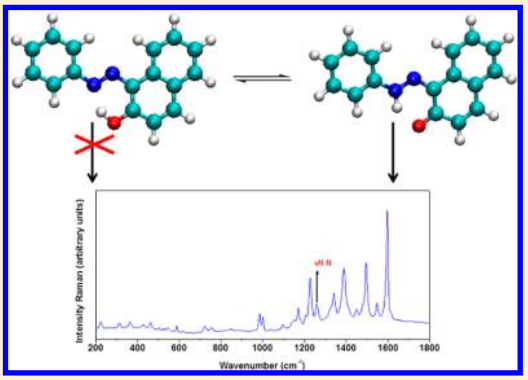

INTRODUCTION

Azo compounds are an interesting class of organic compounds that have found wide application as acid−base, redox, metallochrome, and other indicators. Dyes are also found in food, pharmaceutical, paints, polymers, and standard materials used in adsorption chromatography.[1] About 50% of the dyes produced in the world are derived from azo compounds. The main characteristic of this family of compounds is the presence of the azo group (−N═N−), which allows larger extension of π-electronic conjugation and, therefore, intense absorption of light in the visible region of the electromagnetic spectrum.[2] Azo dyes are also of particular interest to chemists, because they can be easily prepared with a wide range of donor and acceptor groups and also because the planarity of the azo bridge is expected to promote electronic delocalization, increasing the absorption strength.[3−6] In the case of azo-2-naphthol derivatives, a strong hydrogen bond enhanced by resonance is established, inducing the azo (OH) → hydrazo (NH) tautomeric displacement.

The structures of numerous azo compounds have been investigated by several techniques such as Raman, resonance Raman, infrared (IR), and nuclear magnetic resonance (NMR).[7−12] Nonetheless, the precise assignments of the spectroscopic signs are still incomplete regarding the tautomers composition (OH/NH) in the medium. In this study, we present an extensive experimental and theoretical investigation of the 1-phenyl-azo-2-naphthol (also known as Solvent Yellow 14 or Sudan I) and three more derivatives: 1-(2,4-xylyl-azo)-2-naphthol (Solvent Orange 7 or Sudan II), 1-(*p*-nitrophenyl-azo)-2-naphthol (Para Red), and 1-(2-methoxyphenyl-azo)-2-naphthol (also known as Oil Red 113 or Sudan Red G) (Figure 1). Several spectroscopic techniques are used, Raman, UV/visible, infrared, NMR, and X-ray diffraction, in addition to quantum chemical methods. On the basis of the spectroscopic and theoretical data, the azo/hydrazo equilibrium is discussed for the series of Sudan I analogues.

EXPERIMENTAL SECTION

Materials and Experimental Methods. All azo compounds were purchased from Aldrich with purity of 97% for Sudan I, 90% for Sudan II, and 95% for the Para Red and Sudan red G, and were used without any further treatment. The solvents used were spectroscopic grade. Raman spectra were obtained from the solid phase, using a Bruker RFS 100 FT-Raman instrument equipped with germanium detector refrigerated by liquid nitrogen, with excitation at 1064 nm from a Nd:YAG laser, power between 20 and 60 mW for sample in the solid phase, in the range between 4000 and 50 cm^{-1}, and spectral resolution of 4 cm^{-1}, with an average of 500 scans. Infrared (IR) spectra were recorded in a Bomem FTIR MB102 spectrometer, in the region 4000−50 cm^{-1} of the sample supported at KBr pellet, with 4 cm^{-1} of spectral resolution, and an average of 64 scans. The electronic spectra were obtained in a Shimadzu UVPC 1601 spectrophotometer using 10.0 mm quartz cuvets and the solvents ethyl ether, *n*-hexane, chloroform, dichloromethane, ethyl acetate, and ethanol. The ^{13}C NMR and ^{1}H spectra were obtained using a Bruker AC-300 operating in the 75.43 MHz frequency range, using $CDCl_3$ for spectral acquisition and NMR quartz tube of 5

Received: October 16, 2012
Revised: January 4, 2013
Published: January 5, 2013

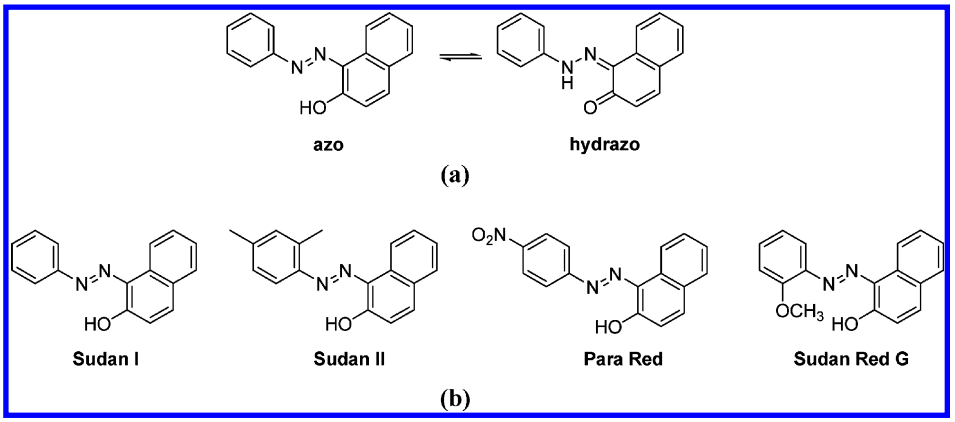

Figure 1. (a) Structures for azo (OH) and hydrazo (NH) forms of Sudan I. (b) The Sudan I derivatives studied here.

mm of diameter. The chemical shifts δ (ppm) were obtained from comparison using TMS as internal standard. Single crystal X-ray data were collected using an Oxford GEMINI A Ultra diffractometer with MoKα (λ = 0.71073 Å) at room temperature (298 K) for Sudan I. Data collection, reduction, and cell refinement were performed by CrysAlis RED, Oxford Diffraction Ltd.,[13] Version 1.171.32.38. The structures were determined and refined using SHELXL-97.[14] The empirical isotropic extinction parameter x was refined according to the method previously described by Larson,[15] and a Multiscan absorption correction was applied.[16] The structures were drawn by ORTEP-3 for Windows[17] and Mercury[18] programs. CCDC 842862 contains the supplementary crystallographic data for Sudan I. These data can be obtained free of charge at http://www.ccdc.cam.ac.uk or from the Cambridge Crystallographic Data Centre, 12 Union Road, Cambridge CB2 IEZ, UK [fax (Internet), 1 44-1223/336−033; e-mail, deposit@ccdc.cam.ac.uk].

Calculations. The structures for the OH and NH isomers (Figure 1) were optimized in the gas phase at B3LYP[19,20] level using the 6-311++G(d,p)[21] triple-ζ quality basis set (hereafter abbreviated as B3LYP/6-311++G(d,p)). The final geometries were characterized as minima on the potential energy surface (PES) through harmonic frequencies calculation (all frequencies found real). The IR and Raman spectra were calculated and the band spectra simulated by fitting a Lorentzian type function,[22] with parameters set to 10 cm^{-1} for the average width of the peaks at half height and 2×10^{-6} mol cm^{-3} for sample concentration. The spectra for all species were then assigned according to the normal mode visualization. Frequency scaling was not needed once predicted values and spectrum profile were in satisfactory agreement with the experiment, allowing unambiguous band assignments. The ^{13}C and ^{1}H NMR spectra were calculated at B3LYP/6-311++G(d,p) level in chloroform solution, with the solvent effect included through the PCM continuum model[23] with macroscopic dielectric constant set to 4.71 (chloroform solution). The gauge-independent atomic orbital (GIAO) method[24] was used to predict the ^{13}C and ^{1}H magnetic shielding constants (σ) with chemical shifts (δ) obtained on a δ scale relative to TMS, taken as reference. Last, the UV/vis transitions were also calculated and assigned in chloroform solution for both forms using the time-dependent (TD) approach[25,26] at B3LYP/6-311++G(d,p) level of theory. As done for Raman spectra, the UV/vis band shape was also simulated by fitting a Gaussian type function,[27] to allow a direct comparison with experimental spectra. The use of Gaussian gives a better match to the observed UV/vis spectra for such wide bands. All calculations were carried out with Gaussian 09 program[28] as installed in the computers at the Núcleo de Estudos em Química Computacional (NEQC-UFJF).

RESULTS AND DISCUSSION

X-ray Diffraction Measurements for Sudan I Parent Compound. The crystal structure of Sudan I was reported several years ago in three independent studies.[29−31] These studies showed a C-centered monoclinic structure with different space groups $C2/C$, $C2/C$, and $P2_1/C$ (volumes 2519, 2434, and 2486 $Å^3$) and the number of repeat units in the unit cells equal to eight. The density was 1.309, 1.355, and 1.33 g/cm^3, respectively, and the crystals were diffracted at different temperatures of 300, 213, and 173 K.

The new crystals of Sudan I were obtained in a test tube from a saturated solution in dichloromethane through the slow evaporation of the solvent; the crystals were dried and separated for analysis of X-ray diffraction. We found that the new structure is slightly different from those previously reported for Sudan I.[29−31] The thermal ellipsoid representation of this new structure is shown in Figure 2. Sudan I crystallizes

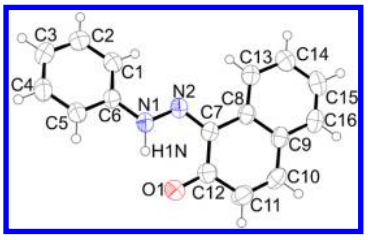

Figure 2. Thermal ellipsoid representation of $C_{16}H_{12}N_2O$ showing the atom labeling scheme. The thermal ellipsoids are scaled to the 50% probability level. Hydrogen atoms are drawn to an arbitrary scale.

in the monoclinic system, space group $P2_1/C$, with four repeating units. This structure revealed an inversion center in the center and one rotation axis 2_1 along the axis C as shown in Figure 3. The crystallographic refinements are listed in Table 1, whereas bond lengths and bond angles are shown in Table 2.

The reported crystallographic structure in this same monoclinic system was found to be planar.[31,32] However, the structure described here shows torsion of 15.15° and 164.44° for the dihedral angles $N_2N_1C_6C_1$ and $N_2N_1C_6C_5$, respectively. These torsions affect the overall crystallographic arrangement

dx.doi.org/10.1021/jp310229h | J. Phys. Chem. A 2013, 117, 642−649

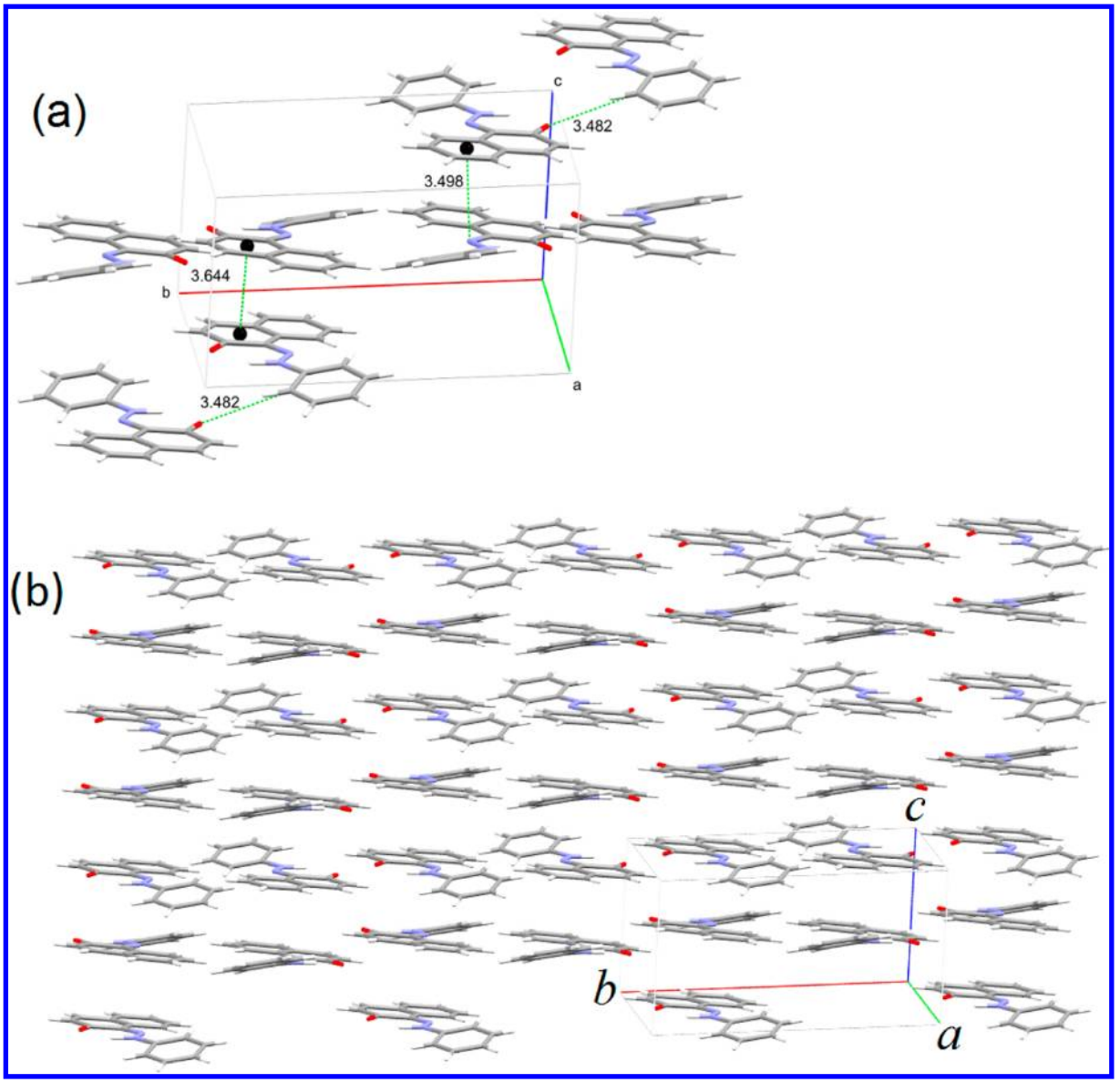

Figure 3. Supramolecular interactions CH···O, π-stacking, and charge dipole were parallel to the *ab* plane for Sudan I: (a) unit cell and (b) bidimensional arrangement.

by creating two adjacent planes in relation to the naphthol ring and to the phenyl ring (Figure 3a). The solid-state arrangement displays supramolecular interactions of the π-stacking type between the two adjacent rings of the naphthol group, which can be better seen in Figure 3a and b. The distance between two centroids is 3.644 Å, which is of the same order as found previously,[33] and the naphthol rings are aligned perpendicularly with the dihedral defined by the four centroids in the naphthol rings equal to 101°. Intramolecular interactions are observed between hydrogen atoms $N_1\cdots H_\alpha\cdots O_1$ forming a six-member ring. The distance between the donor−acceptor groups ($N_1\cdots O_1$) is 2.5284 Å. Although this distance is shorter than the π-stacking observed between the centroids of the naphthol groups, the latter is notably important for packaging the crystalline structure.[34−38] Another type of π-stacking interaction is also noted in the structure described here. The adjacent molecules are arranged so that the naphthol ring is approximately centered over azo moiety, with the N_1 and N_2 distances from the centroid of the aromatic ring found to be 3.648 and 3.498 Å, respectively, and the angle between the centroid and the N_1N_2 equal to 20.75°. The packing results in columns of π-stacking molecules extending alongside the *c* axis. This type of interaction, dipole−dipole in nature, seems to be much stronger than centroids−centroids interaction, which is purely induced-dipole in nature. Unconventional hydrogen bonds of type CH···O are also observed between adjacent molecules with the distance between the carbon and oxygen found to be 3.482 Å (see Figure 3a).

Structures and Energies for Sudan I and Their Derivatives. Molecular modeling based on DFT calculation was used to predict structure, energy, and spectroscopic properties for Sudan I and the other three derivatives shown in Figure 1. The B3LYP/6-311++G(d,p) optimized geometries for all compounds studied in the OH and NH forms are given in Figure S1 as Supporting Information. Table 3 reports the predicted structural parameters for Sudan I only, for which experimental data are available. For Sudan II, Sudan Red G, and Para Red, the calculated structures were close to that of Sudan

dx.doi.org/10.1021/jp310229h | J. Phys. Chem. A 2013, 117, 642−649

Table 1. Crystallographic Data and Details of the Structure Refinement for Sudan I

compound	Sudan I
formula	$C_{16}H_{12}N_2O$
formula weight/g mol^{-1}	248.28
crystal system	monoclinic
space group	$P21/c$
a/Å	13.0665(5)
b/Å	13.4920(5)
c/Å	6.9980(3)
α/deg	90.00
β/deg	94.179(4)
γ/deg	90.00
V/Å^3	1230.42(8)
Z	4
crystal size/mm	0.82 × 0.30 × 0.20
D_{calc}/g cm^{-3}	1.340
μ(Mo Kα)/cm^{-1}	0.086
transmission factors (min/max)	0.969/0.983
reflections measured/unique	5327/2521
observed reflections [$F_o^2 > 2\sigma(F_o^2)$]	1706
no. of parameters refined	177
$R[F_o > 2\sigma(F_o)]$	0.0420
$wR[F_o^2 > 2\sigma(F_o)^2]$	0.1102
S	0.953
RMS peak	0.069

Table 2. Selected Geometrical Parameters of Sudan I in the Solid State

bond angle/deg		bond lengths/Å	
$N_1-N_2-C_7$	117.72 (0.10)	N_2-C_7	1.3471 (0.0014)
$N_2-N_1-C_6$	119.69 (0.10)	N_1-N_2	1.2957(0.0013)
$N_2-C_7-C_8$	116.47 (0.10)	N_1-C_6	1.4048 (0.0014)
$N_2-C_7-C_{12}$	123.58 (0.10)	O_1-C_{12}	1.2773 (0.0014)
$N_1-C_6-C_1$	122.89 (0.10)	$C_{11}-C_{12}$	1.4291 (0.0017)
$N_1-C_6-C_5$	120.15 (0.11)	$C_{11}-C_{10}$	1.3417 (0.0018)
$C_7-C_{12}-O_1$	121.76 (0.10)	C_9-C_8	1.4106 (0.0016)
$C_7-C_8-C_9$	122.60 (0.10)	C_9-C_{16}	1.3954 (0.0017)
$C_{10}-C_{11}-C_{12}$	121.69 (0.12)	C_9-C_{10}	1.4370 (0.0018)
$O_1-C_{12}-C_{11}$	120.36 (0.11)	C_9-C_{16}	1.3954 (0.0017)
$C_4-C_5-C_6$	119.69 (0.12)	$C_{11}-C_{10}$	1.3763 (0.0017)

I, with the effects of the donor and acceptor groups found localized close to the substituent position. The structural parameters for these molecules are given as Supporting Information (Tables S1−S3). Analyzing the dihedral angles of the azo-compound around the N_1-N_2 bond, it can be noted that the structures for isolated molecules are planar (all dihedral angles in Table 3 are 0° or 180°). The planarity of molecules favors a strong intramolecular hydrogen bond. The predicted $O_1-H\alpha\cdots N_1$ (OH) and $N_1-H\alpha\cdots O_1$ (NH) distances for the compounds Sudan I, Sudan II, Para Red, and Sudan Red G are, respectively, 1.66, 1.65, 1.65, and 1.64 Å for the OH form, and 1.71, 1.68, 1.72, and 1.74 Å for the NH isomer. These distances are significantly smaller than the summation of the van der Waals radii (~2.6 Å), just confirming the existence of a very strong hydrogen bond in all of these compounds. The $N_1\cdots O_1$ distance is approximately 2.54 Å, very close to the experimental value obtained for Sudan I, 2.5284 Å. The short distances can be interpreted by means of the high degree of electronic delocalization present in both tautomers and can be analyzed in terms of the resonance forms. Hydrogen bonds are usually strong when they are involved in resonance, and several effects on the chemical and physical properties can be observed, such as the decrease in the force constants of the N−H, O−H, or C═O bonds, leading to a decrease of the vibrational frequencies. The relative Gibbs free energy calculated in the gas phase for the OH→NH conversion process favors, in general, the NH tautomer by (ΔG in kcal mol^{-1}) −1.05 kcal mol^{-1} for Sudan I, −1.70 for Para Red, and −1.99 for Sudan Red G. The corresponding value for Sudan II was 0.63 kcal/mol favoring the OH tautomer at B3LYP/6-311++G(d,p). The relative Gibbs free energy was also calculated in solution where the solvents are characterized by their dielectric constant: *n*-hexane (ε = 1.88), ethyl ether (ε = 4.24), chloroform (ε = 4.71), ethyl acetate (ε = 5.98), dichloromethane (ε = 8.93), and ethanol (ε = 24.85). The Gibbs free energy values for all processes are given as Supporting Information (Table S4). Analyzing the results, it is clear that when the dielectric constant increases, the NH tautomer is favored. It is also worth noting from the values in Table S4 that the solvent effect is more pronounced up to ε = 5 and converges quickly with dielectric constant increasing. Therefore, significant changes in the tautomer population are not expected in polar solvents, such as DMSO or water.

Spectroscopic Analysis. The IR and Raman spectra were calculated for both OH and NH species and used to assign the experimental bands. The measured spectra are given in Figure 4 with wavenumber and assignments of the main bands quoted in Tables 4 (IR) and 5 (Raman). Despite the quite complex profile of the vibrational bands, some fingerprints can be

Table 3. Optimized Geometric Parameters for the Tautomeric Forms (OH and NH) of Sudan I Calculated at the B3LYP/6-311++G(d,p) Level in the Gas Phase

bond angle/deg	OH	NH	dihedral angles/deg	OH	NH	bond lengths/Å	OH	NH
$N_1-N_2-C_7$	117	120	$N_1-N_2-C_7-C_{12}$	0	0	$H_\alpha-O_1$	1.0	1.71
$N_2-N_1-C_6$	116	121	$N_1-N_2-C_7-C_8$	180	180	N_1-N_2	1.27	1.3
$N_2-C_7-C_8$	116	116	$N_2-N_1-C_6-C_1$	0	0	$H_\alpha-N_1$	1.66	1.0
$N_2-C_7-C_{12}$	123	122	$N_2-N_1-C_6-C_5$	180	180	N_2-C_7	138	1.32
$N_1-C_6-C_1$	124	122	$N_2-C_7-C_8-C_{13}$	0	0	N_1-C_6	1.41	1.40
$N_1-C_6-C_5$	126	117	$O_1-C_{12}-C_7-C_8$	180	180	N_1-H_α	2.34	1.92
$C_7-C_{12}-O_1$	122	122	$N_1-C_6-C_1-C_2$	180	180			
$C_7-C_8-C_9$	122	122	$N_1-C_6-C_5-C_4$	180	180			
$C_7-C_8-C_9$	119	118	$C_7-N_2-N_1-C_6$	180	180			
$O_1-C_{12}-C_{11}$	117	121	$N_2-C_7-C_{12}-O_1$	0	0			
$O_1-H_\alpha-N_1$	144	136	$C_7-C_{12}-O_1-H_\alpha$	0	0			

dx.doi.org/10.1021/jp310229h | J. Phys. Chem. A 2013, 117, 642−649

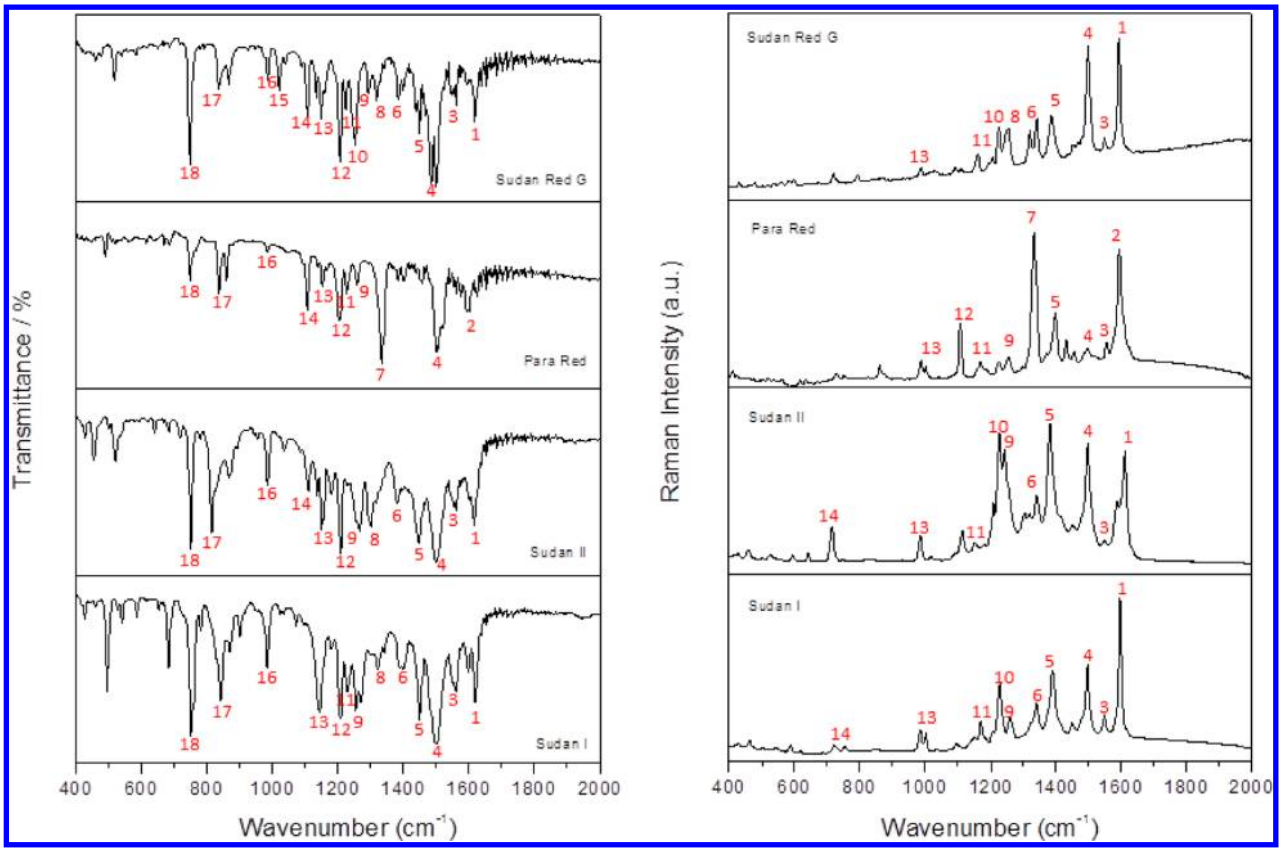

Figure 4. IR and Raman experimental spectra for Sudan derivatives in the solid state.

Table 4. Wavenumber (in cm^{-1}) and Assignments of the Main IR Absorption Bands Observed for the Azo Dyes Derivatives[a]

	Sudan I	Sudan II	Para Red	Sudan Red G	assignments
1	1618	1616		1618	δNH, ν_sCC, δCH
2			1595		ν_sCC, δCH, $\nu_s NO_2$
3	1560	1560		1560	δNH, ν_sC═O
4	1500	1500	1500	1500/1485	δNH, ν_sC═N
5	1448	1448		1448	δCH
6	1400	1382		1384	ν_sC═N, ν_sCC, δCH
7			1332		ν_sC−NO_2, δNH, ν_sCC
8	1323	1301		1319	ν_sCC, δCH
9	1255/1269	1267	1259	1294	ν_sNN, δNH
10				1253	δNH, ν_sCC, δCH, ν_sNN, ν_sC−OCH_3
11	1228		1227	1224	ν_sCC, δCH, ν_sC−NH
12	1207	1209	1205	1207	ν_sCC, δCH
13	1143	1151	1153	1149	ν_sCC, δCH
14		1110	1107	1108	ν_sCC, δCH
15				1020	ν_sO−CH_3
16	985	985	985	987	δCCC
17	842	814	837	837	ωNH
18	752	752	748	750	ωCH

[a]The numbering sequence used for the absorption bands is represented in Figure 4. Nomenclature: δ, in-plane angular deformation; ν_s, stretching; ω, out-of-plane deformation.

identified, and all of them suggest the presence of NH isomer in greater proportion in the solid state. In the IR spectra, the presence of intense bands at ∼1500 and ∼840 cm^{-1} (bands 4 and 17 in Figure 4 and Table 4) is mainly due N−H deformation in-plane (with contribution from γ_sC═N) and ωNH out-of-plane, respectively. The absorptions around 1560−1618 cm^{-1} also have contributions from δNH and ν_sC═O, characteristic of NH tautomer.[39] For the Para Red derivative, a strong band at 1332 cm^{-1} (band 7 in Figure 4 and Table 4) is attributed to ν_sC−NO_2, and for Sudan Red G compound the band at 1253 cm^{-1} (band 10 in Figure 4 and Table 4) is assigned to a very complex mode with contribution from ν_sC−OCH_3. Two other characteristic absorptions of NH isomer are found at 1255−1294 cm^{-1} (ν_sN−N, band 9) and 1224−1228 cm^{-1} (ν_sC−NH, band 11), although lower in intensity. Calculated spectra are provided as Supporting Information in Figures S2 and S3. For comparison, Kunov-Kruse et al.[38] have obtained Raman spectra for Sudan I using the 532 nm laser line excitation, both in the solid and in dichloromethane solution; their experimental and theoretical results are in a good agreement with ours, and even though the work was not focused in the determination of the main species present in the dye, the authors conclude that the NH species is the predominant one in the structure of Sudan I.

The assignments of Raman spectra also support the presence of NH tautomer in the solid state for all four azo dyes studied. The bands at 1547−1611 cm^{-1} (bands 1−2 in Figure 4 and Table 5) are mainly due to CC stretching and CH in-plane deformation, which is present in both OH and NH isomers; however, it is significantly intensified when the hydrazo form is present due the contribution from the δNH mode.[39] The intense band at 1382−1397 cm^{-1} (band 5 in Figure 4 and

dx.doi.org/10.1021/jp310229h | J. Phys. Chem. A 2013, 117, 642−649

Table 5. Wavenumber (in cm^{-1}) and Assignments of the Main Raman Bands Observed for the Azo Dyes Derivatives[a]

	Sudan I	Sudan II	Para Red	Sudan Red G	assignments
1	1596	1611/1586		1592	ν_sCC, δCH, δNH
2			1592		ν_sCC, δCH, δNH, $\nu_s NO_2$
3	1547	1547	1554	1498	δNH, γ_sC═N, ν_sC═O
4	1495	1495	1496	1498	ν_sCC, δCH, ν_sC−NH
5	1389	1382	1397	1386	ν_sC═N, δNH, ν_sCC, δCH
6	1341	1341		1341/1321	ν_sCC, δCH
7			1332		ν_sC−NO_2, δNH, ν_sCC
8				1253	δCH, ν_sCC, ν_sC−OCH_3
9	1258	1243	1253		ν_sNN, δNH, ν_sCC, δCH
10	1227	1225	1226	1224	ν_sCC, δCH, ν_sC−NH
11	1169	1152	1168	1160	δCH
12			1108		δCH, ν_sC−NO_2
13	1002/984	984	1002/987	987	δCCC
14	763/722	714			δCCC

[a]The numbering sequence used for the vibrational bands is represented in Figure 4. δ, in-plane angular deformation; γ_s, axial deformation (stretching); ω, out-of-plane deformation.

Table 5) is also assigned to NH species (ν_sC═N, δNH) as well as the weaker bands at 1243−1258 cm^{-1} due to N−N stretching (bands 8 and 9 in Figure 4 and Table 5). The ν_sC−NO_2 mode is also active in the Raman spectrum of Sudan Red G and appears as a very strong band at 1332 cm^{-1}. The Raman spectra of the azo dyes measured in solution of chloroform and dichloromethane do not change significantly and suggest the predominance of the NH tautomer in solution likewise.

The ^{13}C and ^{1}H NMR spectra of the Sudan I derivatives have also been measured in $CHCl_3$ solution. For analysis, the atoms C_6, C_7, C_{12}, C_{11}, and C_{10} were selected because they are directly involved in the azo/hydrazo isomerization and, therefore, are more sensitive to the proton transfer process.[40,41] In addition, the chemical shift for the H_α atom is also provided (see Table 6). The chemical shift of C_{12} in all compounds is the highest among the selected atoms and is between the values for standard ketone (~200 ppm) and phenoxide (~170 ppm) groups (see Table 6). For the molecules analyzed here, the observed values for δC_{12} were (in ppm): 171.78 (Sudan I), 170.64 (Sudan II), 176.95 (Para Red), and 176.06 (Sudan Red G). When compared to the predicted values for the OH and NH forms, we found the chemical shifts calculated for the hydrazo form in better accordance with the observed ones, except for the Sudan II molecule, which should exist in $CHCl_3$ solution as a mixture of OH (43%) and NH (57%) isomers (see Table S4). Interestingly, when the weighted average chemical shifts are calculated for Sudan II, the agreement with experiment becomes excellent, with the average absolute error found around 1 ppm. For the other derivatives, the NH form is predominant in solution with relative concentration higher than 90%; therefore, the chemical shifts for NH isomer are close to the average values and to the experimental data (the average absolute error for these derivatives is in the range of 3−5 ppm).

The UV/visible spectra were recorded in the following solvents: ethanol (ε = 24.85), ethyl ether (ε = 4.24), *n*-hexane (ε = 1.88), dichloromethane (ε = 8.93), chloroform (ε = 4.71), and ethyl acetate (ε = 5.98) (all solvents of analytical grade). The observed spectra are shown in Figure 5. The lowest energy band was monitored for each sample and compared to the theoretical values, calculated in the same solvents. The results for Sudan I parent compound are plotted in Figure S5 as Supporting Information, and clearly show a red-shift from 460 to 480 nm with increase of the dielectric constant of the solvent. Interestingly, the band position does not vary systematically with strength of solvent effect, with $CHCl_3$ providing the highest red-shift (~23 nm) and ethyl acetate a smaller effect than CH_2Cl_2. The observed trend is satisfactorily reproduced by the theory for both isomers, with absolute values for NH isomer in closer accordance with experiment except for Para Red. The sensitivity of band position is less pronounced in the calculated values due, mainly, to the lack of specific interactions within the PCM formalism; however, the bulk effect is accounted for and seems to be relevant for the overall solvent effect.

Table 6. Experimental and Calculated ^{13}C and ^{1}H NMR Chemical Shifts (ppm) and Assignments for Sudan I, Sudan II, Para Red, and Sudan Red G in $CDCl_3$ Solution[a]

atom	H_α	C_{10}	C_{11}	C_{12}	C_7	C_6
Sudan I exp	**16.24**	**140.78**	**121.88**	**171.78**	**128.24**	**145.05**
NH	16.81	146.18	128.68	182.95	133.22	145.93
OH	15.35	139.94	120.74	157.61	132.71	155.43
96%NH + 4%OH	16.75	145.93	128.36	181.94	133.20	146.31
Sudan II exp	**16.55**	**139.41**	**121.72**	**170.64**	**133.72**	**141.64**
NH	17.55	140.95	128.78	181.33	133.38	140.74
OH	15.48	138.05	120.83	156.22	133.99	150.47
57%NH + 43%OH	16.66	139.70	125.36	170.53	133.64	144.92
Para Red exp	**16.60**	**140.95**	**121.89**	**176.95**	**128.10**	**149.97**
NH	16.56	148.80	128.10	184.43	135.80	152.22
OH	15.54	144.18	120.16	158.68	134.88	160.32
99%NH + 1%OH	16.55	148.75	128.02	184.17	135.79	152.30
Sudan Red-G exp	**16.57**	**141.04**	**125.92**	**177.06**	**127.97**	**132.58**
NH	16.29	145.64	129.67	182.39	133.53	134.84
OH	15.44	139.16	121.93	157.31	133.73	143.51
99%NH + 1%OH	16.28	145.58	129.59	182.14	133.53	134.93

[a]The weighted average values are also included for each compound where the Gibbs population is used as weight.

dx.doi.org/10.1021/jp310229h | J. Phys. Chem. A 2013, 117, 642−649

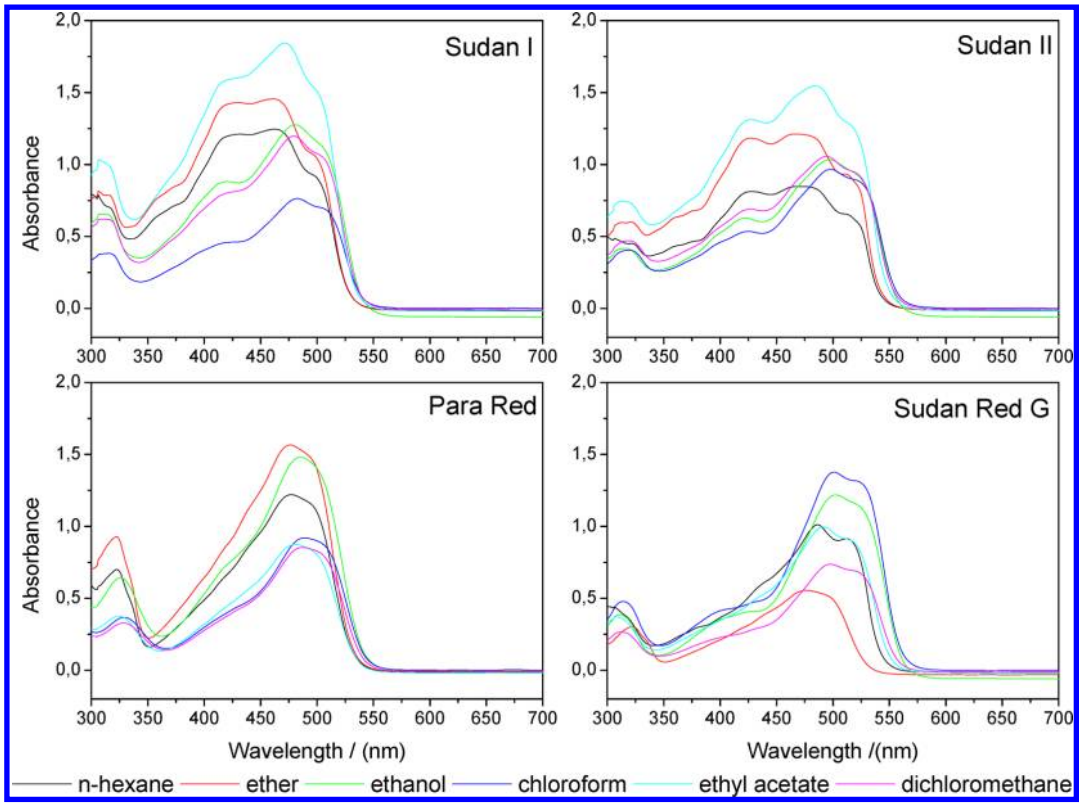

Figure 5. Experimental UV−visible spectrum obtained for Sudan I, Sudan II, Para Red, and Sudan Red G dyes in *n*-hexane, ether, ethanol, chloroform, ethyl acetate, and dichloromethane.

CONCLUSIONS

The new X-ray structure for Sudan I showed the presence of the NH tautomer in the solid state; weak intermolecular interactions were observed, such as π-stacking and hydrogen bonding of the unconventional type C−H···O. For all derivatives studied, the infrared and Raman spectra were assigned with the aid of normal-mode analysis and also suggest the hydrazo form as predominant. In the IR spectra, intense bands are assigned to N−H deformation at ca. 1500 and 840 cm^{-1}. The former is also observed in the Raman spectra in addition to an intense band around 1400 cm^{-1} due to C═N stretching. The analysis in solution by NMR spectroscopy supports the presence of NH isomer. For Sudan I, the observed NMR chemical shifts (in $CHCl_3$) for Hα and C12 were 16.2 and 171.8 ppm, which characterize the hydrazo form, if we compare to the corresponding predicted values of 16.8 and 182.9 ppm for NH isomer and 15.4 and 157.6 ppm for OH isomer. To sum, all of the spectroscopic and theoretical results show that the Sudan family of compounds presents the "hydrazo" structure as the prevalent, when compared to the "azo" form, mainly in highly polarizable solvents.

ASSOCIATED CONTENT

Supporting Information

Figure S1 shows the optimized geometries for all of the studied compounds in the OH and NH forms at B3LYP/6-311++G(d,p) theory level. Figures S2 and S3 show the infrared and Raman spectrum calculated for all compounds at B3LYP/6-311G ++G(d,p) level of theory. Figure S4 shows the lowest energy transition observed in the UV/vis spectrum of Sudan I in distinct solvents. Tables S1, S2, and S3 display the structural parameters for the tautomeric forms (OH and NH) of Sudan II, Para Red, and Sudan red G, calculated at the B3LYP/6-311++G(d,p) level, and Table S4 shows the relative Gibbs free energy and population for OH/NH species in several solvents. Table S5 shows the wavenumber, oscillator strength, and assignments for the lowest energy transition calculated for Sudan I derivatives in both OH and NH forms. This material is available free of charge via the Internet at http://pubs.acs.org.

AUTHOR INFORMATION

Corresponding Author

*Phone: +55 (32) 3229-3310. Fax: +55 (32) 3229-3310. E-mail: luiz.oliveira@ufjf.edu.br.

Notes

The authors declare no competing financial interest.

ACKNOWLEDGMENTS

We thank CNPq, CAPES, FAPEMIG (PRONEX 526/07, CEX-APQ-00617), and FINEP (PROINFRA 1124/06) for financial support and LabCri (Departamento de Física, UFMG) for the X-ray facilities. This work is a collaboration research project of members of the Rede Mineira de Química (RQ-MG) supported by FAPEMIG (PROCESSO no. REDE-113/10).

REFERENCES

(1) Bershtein, I. Y.; Ginzburg, O. *Russ. Chem. Rev.* **1972**, *41*, 97−110.
(2) Almeida, M. R.; Stephani, R.; Dos Santos, H. F.; de Oliveira, L. F. C. *J. Phys. Chem. A* **2010**, *114*, 526−534.
(3) Snehalatha, M.; Sekar, N.; Jayakumar, V. S.; Joe, I. H. *Spectrochim. Acta, Part A* **2008**, *69*, 82−90.
(4) Yesodha, S. K.; Sadashiva Pillai, C. K.; Tsutsumi, N. *Prog. Polym. Sci.* **2004**, *29*, 45−74.
(5) Towns, A. D. *Dyes Pigm.* **1999**, *42*, 3−28.

(6) Kanis, D. R.; Ratner, M. A.; Marks, T. J. *Chem. Rev.* **1994**, *94*, 195−242.
(7) Bell, S.; Bisset, A.; Dines, T. J. *J. Raman Spectrosc.* **1998**, *29*, 447−462.
(8) Gilli, P.; Bertolasi, V.; Pretto, L.; Lyčka, A.; Gilli, G. *J. Am. Chem. Soc.* **2002**, *124*, 13554−13567.
(9) Alarcón, S. H.; Olivieri, A. C.; Sanz, D.; Claramunt, R. M.; Elguero, J. *J. Mol. Struct.* **2004**, *705*, 1−3.
(10) Fabian, W. M. F.; Antonov, L.; Nedeltcheva, D.; Kamounah, F. S.; Taylor, P. J. *J. Phys. Chem. A* **2004**, *108*, 7603−7612.
(11) Antonov, L.; Fabian, W. M. F.; Taylor, P. J. *J. Phys. Org. Chem.* **2005**, *18*, 1169−1175.
(12) Dos Santos, H. F.; de Oliveira, L. F. C.; Dantas, S. O.; Santos, P. S.; De Almeida, W. B. *Int. J. Quantum Chem.* **2000**, *80*, 1076−1086.
(13) *CryAlis RED. Version 1.171.32.38*; Oxford Diffraction Ltd.: Oxford, UK, 2008.
(14) Sheldrick, G. M. *A Program for Crystal Structure Refinement*; University of Goettingen, Goettingen: Germany, 1997.
(15) Larson, A. C. *Crystallographic Computing*; Carleton University: Copenhagen, Munksgaard, Denmark, 1969; pp 291−294.
(16) Blessing, R. H. *Acta Crystallogr., Sect. A* **1995**, *51*, 33−38.
(17) Farrugia, L. J. *J. Appl. Crystallogr.* **1997**, *30*, 565−565.
(18) Macrae, C.; Edgington, P.; McCabe, P. *J. Appl. Crystallogr.* **2006**, *39*, 453−457.
(19) Becke, A. D. *Phys. Rev. A* **1988**, *38*, 3098−3100.
(20) Lee, C.; Yang, W.; Parr, R. G. *Phys. Rev. B* **1988**, *37*, 785−789.
(21) Gordon, M. S.; Binkley, J. S.; Pople, J. A.; Pietro, W. J.; Hehre, W. J. *J. Am. Chem. Soc.* **1982**, *104*, 2797−2803.
(22) Dos Santos, H. F.; Almeida, W. B. d.; Val, A. M. G. d.; Guimarães, A. C. *Quim. Nova* **1999**, *22*, 732−736.
(23) Cances, E.; Mennucci, B.; Tomasi, J. *J. Chem. Phys.* **1997**, *107*, 3032−3041.
(24) Wolinski, K.; Hinton, J. F.; Pulay, P. *J. Am. Chem. Soc.* **1990**, *112*, 8251−8260.
(25) Karna, S. P.; Dupuis, M. *J. Comput. Chem.* **1991**, *12*, 487−504.
(26) Kurtz, H. A.; Stewart, J. J. P.; Dieter, K. M. *J. Comput. Chem.* **1990**, *11*, 82−87.
(27) De Almedia, W. B.; Costa, L. R. A.; Dos Santos, H. F.; Zerner, M. C. *J. Chem. Soc., Perkin Trans. 2* **1997**, 1335−1339.
(28) Frisch, M. J.; Trucks, G. W.; Schlegel, H. B.; Scuseria, G. E.; Robb, M. A.; Cheeseman, J. R.; Montgomery, J. A.; Vreven, T.; Kudin, K. N.; Burant, J. C.; et al. *Gaussian 09*, revision A01; Gaussian, Inc.: Wallingford, CT, 2009.
(29) Salmén, R.; Malterud, K. E.; Pedersen, B. F. *Acta Chem. Scand.* **1988**, *42*, 493−499.
(30) Olivieri, A. C.; Wilson, R. B.; Paul, I. C.; Curtin, D. Y. *J. Am. Chem. Soc.* **1989**, *111*, 5525−5532.
(31) Chong-Yang, L.; Vincent, L.; Allen, J. B. *Chem. Mater.* **1997**, *9*, 943−949.
(32) Gilli, P.; Bertolasi, V.; Ferretti, V.; Gilli, G. *J. Am. Chem. Soc.* **1994**, *116*, 909−915.
(33) Garcia, H. C.; Diniz, R.; De Oliveira, L. F. C. *CrystEngComm* **2012**, *14*, 1812−1818.
(34) Avvaru, B. S.; Kim, C. U.; Sippel, K. H.; Gruner, S. M.; Agbandje-McKenna, M.; Silverman, D. N.; McKenna, R. *Biochemistry* **2009**, *49*, 249−251.
(35) Ruben, M.; Lehn, J. M.; Muller, P. *Chem. Soc. Rev.* **2006**, *35*, 1056−1067.
(36) Badjić, J. D.; Nelson, A.; Cantrill, S. J.; Turnbull, W. B.; Stoddart, J. F. *Acc. Chem. Res.* **2005**, *38*, 723−732.
(37) Desiraju, G. R. *Acc. Chem. Res.* **2002**, *35*, 565−573.
(38) Bernstein, J.; Davis, R. E.; Shimoni, L.; Chang, N. L. *Angew. Chem., Int. Ed. Engl.* **1995**, *34*, 1555−1573.
(39) Kunov-Kruse, A. J.; Kristensen, S. B.; Liu, C.; Berg, R. W. *J. Raman Spectrosc.* **2011**, *42*, 1470−1478.
(40) Szántay, J. C.; Csepregi, Z.; Aranyosi, P.; Rusznák, I.; Töke, L.; Víg, A. *Magn. Reson. Chem.* **1997**, *35*, 306−310.
(41) Alder, M. J.; Cross, W. I.; Flower, K. R.; Pritchard, R. G. *J. Chem. Soc., Dalton Trans.* **1999**, 2563−2574.